RSC Advances

ROYAL SOCIETY OF CHEMISTRY

www.rsc.org/advances

Elastic properties of carbon nanoscrolls

Mohammad Mahdi Zaeri*, Saeed Ziaei-Rad

Department of Mechanical Engineering, Isfahan University of Technology, Isfahan 8415683111, Iran

E-mail: mm.zaeri@me.iut.ac.ir, Tel: +983115679421

Abstract: The ability to develop mechanical models for nanostructures is of great importance in today's nanotechnology. However, little is known about nanomechanics of several carbon nanostructures other than carbon nanotubes. Here we report a model to predict the elastic properties of one such nanostructure called carbon nanoscroll. The model is based on molecular structural mechanics approach and the properties, including Young's and shear moduli, are sought using finite element method. The influences of geometric parameters such as inner radius, number of turns, length and chirality of carbon nanoscroll on its properties are investigated. Also, the effect of taking van der Waals interactions into consideration is studied. The results indicate that the stiffness of carbon nanoscroll under tension is similar to that of carbon nanotube. However, its torsional stiffness is highly dependent on van der Waals interactions. Without considering van der Waals interactions, shear modulus of carbon nanoscroll is one order of magnitude less than that of carbon nanotube, which is attributed to the open topology of carbon nanoscroll. However, if van der Waals interactions are taken into consideration, both nanostructures have close elastic properties.

Keywords: carbon nanoscrolls, mechanical properties, modeling, molecular structural mechanics, nanomechanics

1. Introduction

Significant achievements in nanotechnology have been obtained in the past three decades such as

discovery of buckyballs and carbon nanotubes (CNTs), invention of atomic force microscope and production of various nanomaterials and nanocomposites. Along with these experimental successes, developing novel theories and models to justify, understand and predict the nanoscale phenomena has been inevitable. In this regard, a great body of knowledge has been developed during the recent years. As an example, many properties of CNTs have been explored and modeled; so that today there is an acceptable literature on them at hand. But there still exist fields requiring considerable research. One such field is the mechanical properties of carbon nanostructures other than CNTs; a good example for which is carbon nanoscroll (CNS).

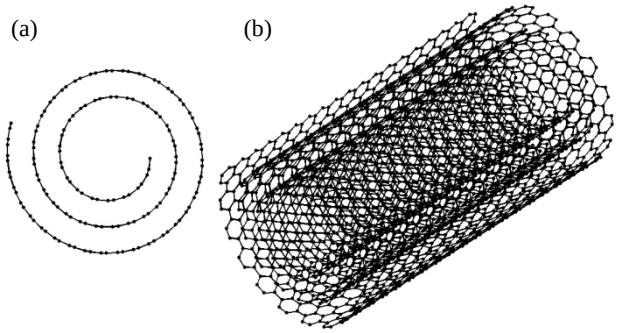

Figure 1: Schematic of a CNS (a) end view (b) 3D view.

As shown in **Figure 1**, CNS is formed by rolling a graphene sheet into a scroll-like structure. It was discovered in 2003[1] and can be used in applications such as hydrogen storage, gigahertz oscillators, nanopumps, nanoactuators, supercapacitors and drug delivery.[2-7] The interlayer spacing of CNS is equal to the van der Waals diameter of carbon, i.e. 0.34 nm, and its inner diameter has a minimum of 1 nm, if it is to be stable.[8-11] Song et al. have performed molecular dynamics simulations of the formation and mechanical behavior of CNS[9]. Among their findings, Young's moduli of 949-972 GPa were obtained. Another research group have studied the electronic properties of CNS and concluded that they are highly chirality-dependent.[11] Using molecular dynamics, Shi et al. have found out that depending on the inside and outside pressure, CNS can expand or contract and hence may be utilized in pressure-sensitive applications such as nanofilter or

nanopump.[4] They also have presented a review on the properties of CNS.[12] Buckling instability of CNS under various loadings has been investigated and compared with CNTs by Zhang et al.[13] They observed that there is no major difference between bending buckling of CNS and CNT. However, under axial compression and torsion, CNS is more prone to buckling. The main difference between CNS and CNT is the open topology of CNS versus the closed topology of CNT. This distinction may cause dissimilar behavior in the two nanostructures, which is discussed in the present paper.

Here, we first develop a mechanical model for CNS and then find out its elastic response under tension and torsion reporting the results in terms of Young's and shear moduli. Also, how the inner radius, number of turns, length and chirality affect the mechanical properties of CNS is investigated. Finally, van der Waals interactions are taken into consideration and their impact is studied.

2. Modeling

2.1. Molecular Structural Mechanics

The modeling method used in this paper is based on Molecular Structural Mechanics (MSM) approach[14] which is briefly explained here. In MSM, the nanostructure is not thought of as a continuum; rather, it is considered as an atomic/molecular structure, as it is in fact. The chemical interatomic and/or intermolecular interactions and bonds are modeled by structural elements like springs, trusses and beams. The mechanical properties of these elements are obtained by setting equal the chemical energies of the bonds and the strain energies of the elements. In carbon nanostructures, carbon atoms play the role of joints or point masses and the bonds between them play the role of structural elements. These bonds may be categorized in three groups: covalent bonds, van der Waals interactions and electrostatic forces. Since CNS only consists of carbon atoms in hexagonal rings, no electrostatic force need be considered. Also, in this paper the elastic

properties are sought, thus the problem is quasistatic and no mass need be defined.

The carbon-carbon covalent bonds are replaced by 3D beam elements because they form only at a certain distance between atoms and can stand tension, bending and torsion. The tensile, bending and torsional constants for a carbon-carbon bond are 652 nN/nm, 0.876 nN.nm/rad^2 and 0.278 nN.nm/rad^2 respectively.[15] Following the above-mentioned procedure one finds the properties of the beam element as $d = 0.1466$ nm, $E = 5488$ nN/nm^2 and $G = 871.1$ nN/nm^2, where d is the beam diameter, E is its Young's modulus and G is its shear modulus. In finding these values the carbon-carbon bond length, or equivalently the beam length, is set to 0.142 nm.[16]

As van der Waals interactions act over a wide range of distances between atoms and are severely nonlinear, they are replaced by nonlinear spring elements. The well-known Lennard-Jones potential function is chosen for van der Waals interaction which is defined as:[17]

$$U(r) = 4\varepsilon\left[\left(\frac{\sigma}{r}\right)^{12} - \left(\frac{\sigma}{r}\right)^{6}\right] \quad (1)$$

where U is the potential energy, r is the distance between atoms and, ε and σ are constants. For carbon, $\varepsilon = 0.00038593$ nN.nm and $\sigma = 0.34$ nm.[18] The force-displacement relation of the spring element is found, through the gradient of the potential energy, as:

$$F(x) = -24\frac{\varepsilon}{\sigma}\left[2\left(\frac{\sigma}{x + \sqrt[6]{2}\sigma}\right)^{13} - \left(\frac{\sigma}{x + \sqrt[6]{2}\sigma}\right)^{7}\right] \quad (2)$$

where F is the force and $x = r - \sqrt[6]{2}\sigma$ is the displacement of the spring from its equilibrium position (free length) of $r = \sqrt[6]{2}\sigma = 0.38$ nm. This relation is depicted in **Figure 2**.

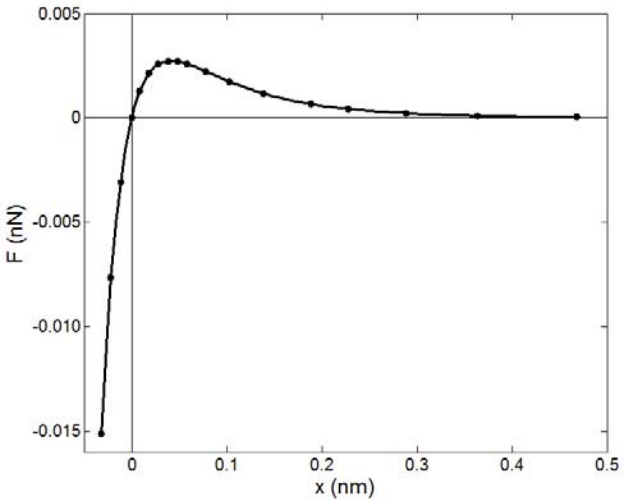

Figure 2: Force-displacement relation for nonlinear spring element.

As can be seen in Figure 2, van der Waals force attenuates for large displacements; therefore a cut-off radius of $r = 2.5\sigma = 0.85$ nm,[19] equivalent to a displacement of $x = 0.47$ nm, is intended beyond which no force is applied. That is, van der Waals interaction is considered to exist between atoms that are within a distance of 0.85 nm from each other. In our models, for the sake of clarity, van der Waals bonds were formed only between adjacent layers. Since these bonds are far weaker than covalent bonds inside the layers, and also there exist a huge number of them, neglecting a few percent of van der Waals bonds crossing CNS layers, does not introduce noticeable error in the modeling.

2.2. Geometry

In order to obtain the elastic moduli of CNS, in the first step, Matlab® codes were developed to generate the geometry of CNS. Since the interlayer spacing of CNS is constant, its structure turns out to be an Archimedean spiral[20] as illustrated in **Figure 3**. Several parameters were considered to be adjustable in the codes. These include inner radius, number of turns of the spiral, length and chirality of CNS. In this way, CNSs with any desired geometrical parameters could be constructed.

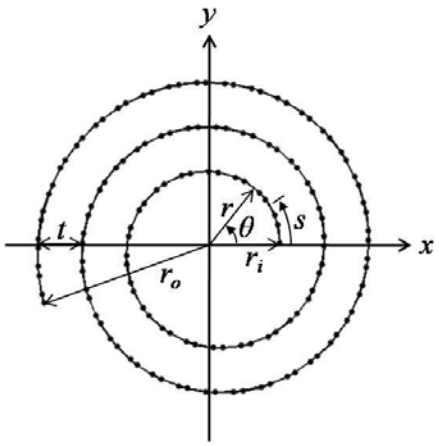

Figure 3: Parameters used to construct the Archimedean spiral of CNS. r_i and r_o are the inner and outer radii respectively, t is the increase in radius per turn of CNS, s is the curve length and, r and θ are the polar coordinates.

Regarding Figure 3, in an Archimedean spiral we have:

$$r = r_i + \frac{t}{2\pi}\theta \tag{3}$$

$$r_o = r_i + n_t t \tag{4}$$

where n_t is the number of turns of the spiral. Using polar equations, the infinitesimal curve length is found to be:

$$ds = \sqrt{\left(r_i + \frac{t}{2\pi}\theta\right)^2 + \left(\frac{t}{2\pi}\right)^2}\, d\theta \tag{5}$$

which can be integrated analytically to derive s, resulting in a lengthy equation. However, if we neglect the very small difference between the radius r of a point on the spiral and the radius of curvature ρ of the spiral in that point, using the arc length formula we may find:

$$ds \approx \left(r_i + \frac{t}{2\pi}\theta\right) d\theta \tag{6}$$

Alternatively, considering t is small relative to r_i, we can imagine that in Equation (5), the second term under radical is very small relative to the first one, hence Equation (5) could be reduced to Equation (6). Integrating the latter, s takes the following simple form:

$$s \approx n_t \pi (2r_i + n_t t) \quad (7)$$

It is worth noting that since in CNS, $t = 0.34$ nm, the minimum inner radius is 0.5 nm and the minimum number of turns is 1, the maximum error of the approximation in Equation (7) equals 0.3%. Thus Equation (7) was used without any significant loss of accuracy.

By running the Matlab® codes, the coordinates of the points representing carbon atoms, and the connecting lines between them, representing bonds, were generated. Then these data were exported to Excel®, and reformed as Ansys® finite element package commands, called Ansys® Parametric Design Language (APDL) commands. In the next step, the commands were imported into Ansys® 13.0 as an input file. Once the geometry was constructed, the lines were defined as beam or spring elements with the properties derived in the previous section and hence CNS was modeled as a 3D structure. For the spring element, the force-displacement relation was given by specifying several points of the diagram as shown in Figure 2. Finally, the nodes on one end of CNS were constrained and the nodes on the other were loaded by axial or torsional loads. Representative pictures of the geometry and loading of CNSs are shown in **Figure 4** and **5** (captured from Ansys® graphical user interface).

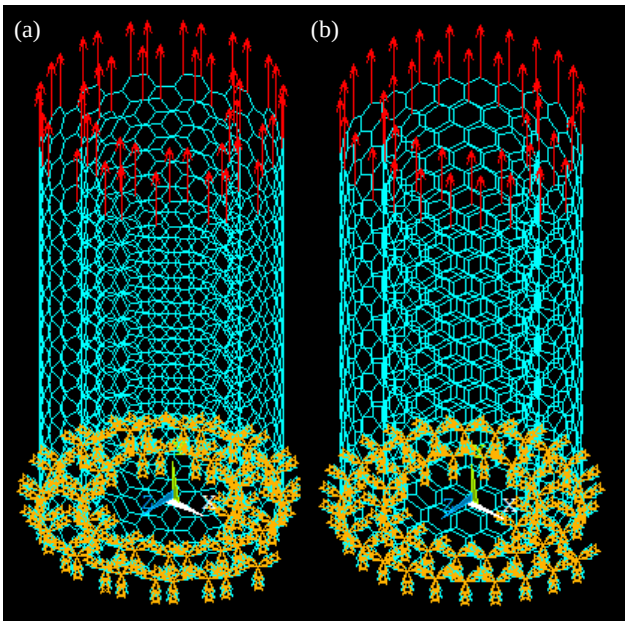

Figure 4: Typical geometry and tensile loading of CNSs without van der Waals interactions (a)

armchair CNS (b) zigzag CNS.

The huge number of van der Waals interactions between layers, compared to the number of covalent bonds inside layers, is noticeable in Figure 5. In models of CNSs without van der Waals bonds, the maximum number of nodes (carbon atoms) is as great as 475,000 and the highest number of beam elements is more than 710,000. Also, in models of CNSs with van der Waals forces, the number of elements hits a maximum of 3,340,000 from which about 85,000 are beam elements and about 3,255,000 are nonlinear spring elements.

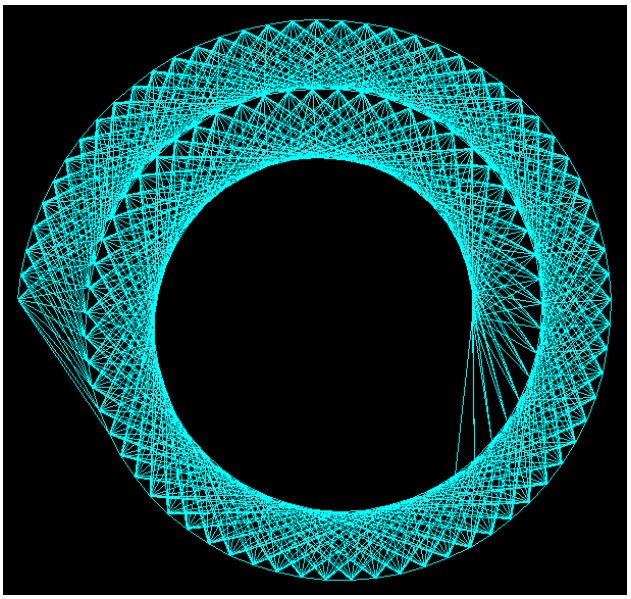

Figure 5: End view of a typical CNS with van der Waals interactions between the atoms of adjacent layers.

Assuming an equivalent continuum model for CNS, its Young's modulus was calculated via the following simple formula from the theory of elasticity:

$$E = \frac{FL}{A\overline{\Delta L}} \tag{8}$$

where E is the Young's modulus, F is the total axial force applied, L is the length of CNS, $\overline{\Delta L}$ is the average displacement of the nodes on the free end of CNS, calculated from the results of the finite

element simulation of tensile loading, and A is the equivalent cross sectional area of CNS. This area is calculated as the total length of the Archimedean spiral, s, times van der Waals diameter of carbon.

Similarly, shear modulus of CNS was derived from finite element simulation under torsional loading. In this case, the torsion formula:

$$G = \frac{TL}{J\overline{\Delta\theta}} \tag{9}$$

was used, in which G is the shear modulus, T is the total torque applied, L is the length of CNS as in Equation (8), $\overline{\Delta\theta}$ is the average angular displacement (twist angle) of the nodes on the free end of CNS and J is the equivalent polar moment of inertia of the cross sectional area of CNS. For calculation of the twist angle, circumferential displacement of each node was divided by its radius to determine the angular displacement, and then the average of the results was calculated. Also, J was calculated via its definition in polar coordinates:

$$J = \int r^2 dA = \iint r^3 dr d\theta \tag{10}$$

Using the parameters already defined and carrying out the integration, one finds:

$$J = \frac{n_t \pi t}{4}[8r_i^3 + 12n_t r_i^2 t + (2 + 8n_t^2) r_i t^2 + (n_t + 2n_t^3) t^3] \tag{11}$$

Interestingly, the geometric equations presented above for CNS, can all be reduced to suitable equations for CNT. In other words, from the geometrical point of view, CNT may be considered as a special case of CNS.

3. Results and Discussion

3.1. Young's Modulus

As stated before, the models studied here are divided into two groups: with and without van der Waals interactions. The results of models without van der Waals forces are presented in the current

and following sections and those of models including van der Waals bonds are presented in Section 3.3.

The results of axial loading simulations of CNSs 20 nm long, having 2.5 turns and varying inner radii and chiralities, namely zigzag and armchair, are shown in **Figure 6**. The least radius is selected to be 0.5 nm since below that, CNS would not be stable. We observe that as the inner radius increases, the values of Young's moduli generally increase and finally converge to a value of 1041 GPa. The increase is due to the increase in the Archimedean curve length of the CNS. As the curve length is increased, the ratio of the nodes far from the two end points of the spiral to the nodes near them increases too. Since the far nodes are less affected by the open topology of CNS, their displacements are smaller than the near nodes. Thus, as the curve length is increased, the average elongation of CNS decreases and results in higher Young's moduli. Also it can be seen that chirality has a small effect on Young's modulus.

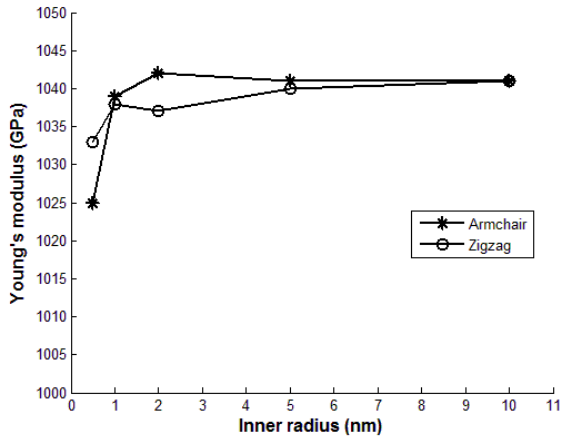

Figure 6: Effect of inner radius on Young's moduli of CNSs (with a length of 20 nm and 2.5 turns).

Figure 7 shows the results of tensile simulations of CNSs 20 nm long, with an inner radius of 1.5 nm and varying number of turns and chiralities. It is seen that Young's moduli increase slightly with the number of turns, converging again to a value of 1041 GPa. The reason for the increase is the same as explained in the previous paragraph, i.e. increase in spiral length. Also again, it is

observed that chirality has no significant effect on Young's modulus (the maximum difference between Young's moduli of similar CNSs having distinct chiralities in Figure 6 and 7 is only 0.8%). It seems that if large enough CNSs are considered (not having very small inner radii or number of turns) chirality does not influence the moduli of CNS, because in such cases the effect of the orientation of individual hexagonal rings on the whole CNS is negligible.

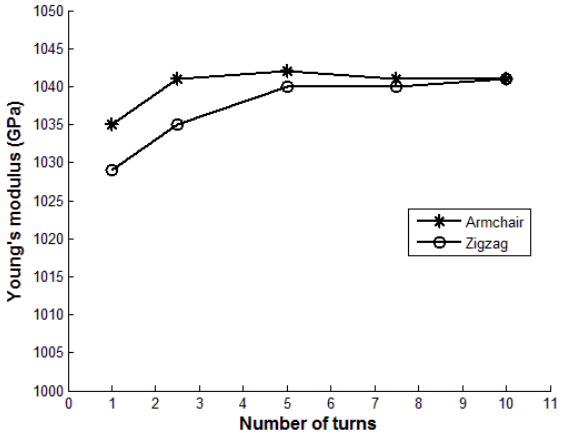

Figure 7: Effect of number of turns on Young's moduli of CNSs (with a length of 20 nm and an inner radius of 1.5 nm).

Finally, the effect of model length on the obtained Young's modulus is depicted in **Figure 8** which summarizes the results of simulations of CNSs having an inner radius of 1.5 nm and 2.5 turns, but with different lengths and chiralities. It shows that short CNSs possess lower Young's moduli, but as length reaches a threshold of about 20 nm, the moduli no more change. Chirality is more prominent here, because the ultimate values of Young's moduli for zigzag and armchair CNSs are different. However, the difference is very small (less than 0.6%) as the Young's modulus for armchair CNS converges to 1042 GPa and that for zigzag CNS converges to 1036 GPa. The orientation of the hexagonal rings with respect to the direction of the applied load can naturally affect the results because the deformation is dependent on the orientation. Furthermore, different chiralities result in slight differences in boundary conditions, because different geometries result in

different number of bottom nodes to be constrained or different number of upper nodes on which the forces are applied. Such small differences cause the moduli to be slightly distinct.

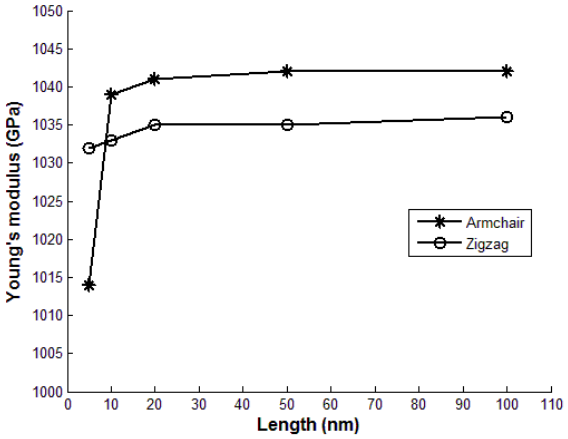

Figure 8: Effect of length on Young's moduli of CNSs (with an inner radius of 1.5 nm and 2.5 turns).

CNSs discussed in literature usually have inner radii greater than 1 nm, numbers of turns less than 8 and lengths greater than 20 nm.[2,4,5,7-13,20,21] Keeping that in mind and comparing the diagrams presented in Figure 6, 7 and 8, a value of around 1040 GPa or 1.04 TPa is predicted to be the Young's modulus of typical CNSs without van der Waals interactions. This is in good agreement with 949-972 GPa for Young's modulus of CNSs obtained from molecular dynamics simulations reported by Song et al.[9] On the other hand, a quick literature review, e.g. see,[14,15,22-25] reveals that the commonly-accepted and well-known Young's modulus for CNTs is about 1 TPa. Therefore one could conclude that the Young's moduli of CNSs and CNTs are nearly the same. This could be intuitively expected, since the open topology of CNS should not influence the longitudinal mechanical properties. The obtained results in the present work verify this expectation.

3.2. Shear Modulus

Diagrams similar to Figure 6, 7 and 8, are prepared for shear moduli of CNSs without van der Waals interactions which present the results of torsional loading simulations. In **Figure 9**, shear moduli of CNSs 20 nm long, having 2.5 turns, with various inner radii and chiralities are presented. Again, the minimum inner radius is 0.5 nm. It can be seen that the moduli change slightly with inner radius in the range of 36-48 GPa. There is nearly no dependence on chirality.

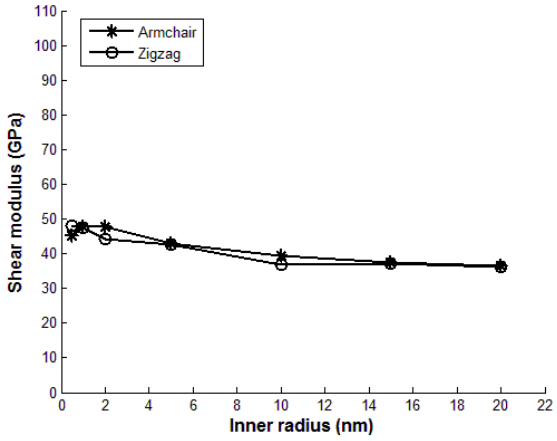

Figure 9: Effect of inner radius on shear moduli of CNSs (with a length of 20 nm and 2.5 turns).

Figure 10 displays the results for CNSs 20 nm long, having an inner radius of 1.5 nm, with varying number of turns and chiralities. In contrast to the previous cases, there is a remarkable dependency between shear modulus and number of turns in this diagram. Shear modulus is notably increased as number of turns increases. This is due to the strength of intermediate layers compared to the weakness of inner and outer layers of CNS. Resistance of the inner and outer layers against torsion is low because they contain the free (open) edges of CNS, while that of intermediate layers is high because they act similar to closed CNTs. Accordingly, as the number of turns increases, the ratio of the strong layers to the weak ones increases, resulting in higher shear moduli. However, the slope of increase gradually decreases, down to near zero eventually. That is because in large numbers of turns, the intermediate layers are dominant and the inner and outer layers' effect is insignificant. According to the diagram, shear modulus adopts a value between 20-100 GPa. Of course, number

of turns of CNSs rarely goes beyond 10 and it is usually less than 5. Therefore, 100 GPa might be considered as an upper limit for shear modulus of CNSs without van der Waals bonds. Once more, it is observed that chirality does not affect the shear moduli.

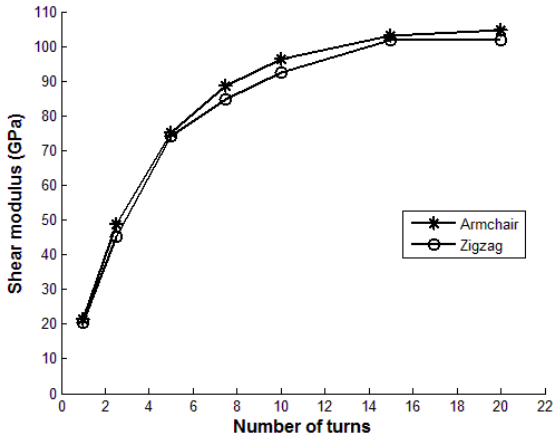

Figure 10: Effect of number of turns on shear moduli of CNSs (with a length of 20 nm and an inner radius of 1.5 nm).

Finally, shear moduli of CNSs with an inner radius of 1.5 nm and 2.5 turns, but with different lengths and chiralities are shown in **Figure 11**. The diagram implies that CNS length also plays an important role. As length increases, the weakening effect of longer inner and outer free edges increases too. Thus the twist angle greatly increases, resulting in poor shear modulus. Suggested by the diagram, in very long CNSs the weakening may be so much that CNS would have slight torsional resistance. By the way, it is repeatedly implied that chirality is not a key parameter in torsional behavior of CNS.

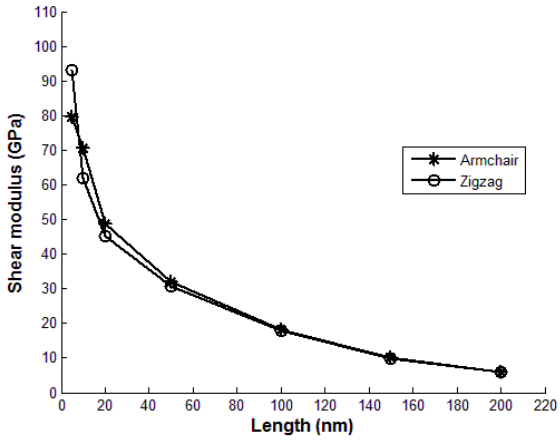

Figure 11: Effect of length on shear moduli of CNSs (with an inner radius of 1.5 nm and 2.5 turns).

Looking after CNSs with geometric parameters discussed in literature, as pointed out in the previous section, one can infer from Figure 9, 10 and 11 that regardless of geometry (inner radius, number of turns, length and chirality), a general value of 40-50 GPa could be suggested as the shear modulus of CNSs without van der Waals forces. A brief literature review[14,15,22-25] implies that shear moduli of CNTs are typically in the range of 350-550 GPa. Therefore shear modulus of a typical CNS, if no van der Waals interaction is considered, is an order of magnitude smaller than that of a typical CNT. This result clearly exhibits the impact of the open topology of CNS in comparison with the closed topology of CNT.

3.3. Effect of van der Waals Interactions

Based on the results of Section 3.1 and 3.2 four sample models, whose elastic properties were close to the conclusions of $E = 1040$ GPa and $G = 40 - 50$ GPa for CNSs without van der Waals bonds, were selected in order to investigate the effect of van der Waals interactions. To do so, in addition to the covalent bonds modeled by beam elements in the simulations of the two previous sections, van der Waals forces were taken into consideration and modeled by nonlinear spring elements. Then, tensile and torsional loadings were applied to the new models (containing both

beam and spring elements) in a similar way as before, and their moduli were compared to the moduli of their old counterparts (containing beam elements only). **Figure 12** and **13** present such comparisons. One can see from Figure 12 that van der Waals forces do not affect the Young's modulus considerably. The maximum increase due to addition of van der Waals interactions is 6%. The reason behind it is that, in tension the interlayer spacing of CNS is not changed considerably. Therefore, van der Waals bonds, existing between layers, do not feel any remarkable change and hence play an insignificant role in calculation of Young's modulus. Also it is seen that as number of turns and length of CNS increase, Young's modulus increases slightly, which is caused by the added number of van der Waals bonds.

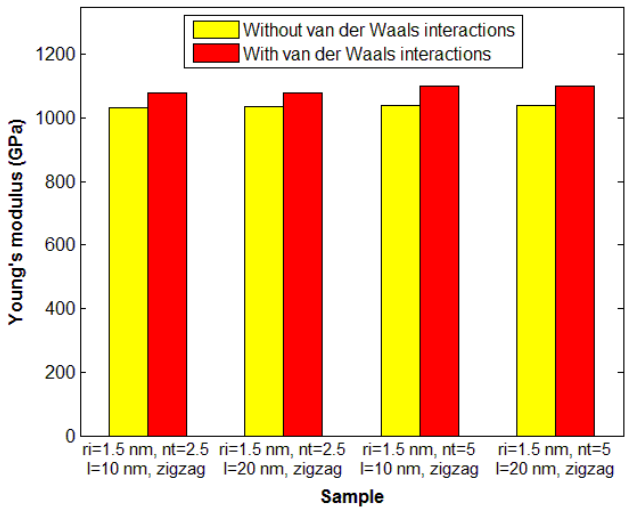

Figure 12: Comparison of Young's moduli of sample CNSs with and without van der Waals interactions (r_i is the inner radius, n_t is the number of turns and l is the length of CNS).

Conversely, Figure 13 demonstrates that the shear modulus extremely depends on van der Waals interactions so that shear modulus of CNSs with van der Waals forces can be up to 10 times greater than that of CNSs without van der Waals forces. This is justified by the interlayer spacing. In contrast to tension, in torsion the interlayer spacing tends to change due to the existence of free edges. If no van der Waals bond between the layers is considered, this tendency is realized, resulting in very low shear modulus. One may imagine that some kind of slip occurs between the

layers. But when van der Waals bonds are taken into consideration, they resist the tendency so that no slip occurs between the layers and CNS stands against the applied torsional load as a whole. Thus the twist angle is decreased and the shear modulus is increased drastically. Furthermore, as number of turns and length of CNS increase, there is a little increase in shear modulus which is due to the added number of van der Waals bonds.

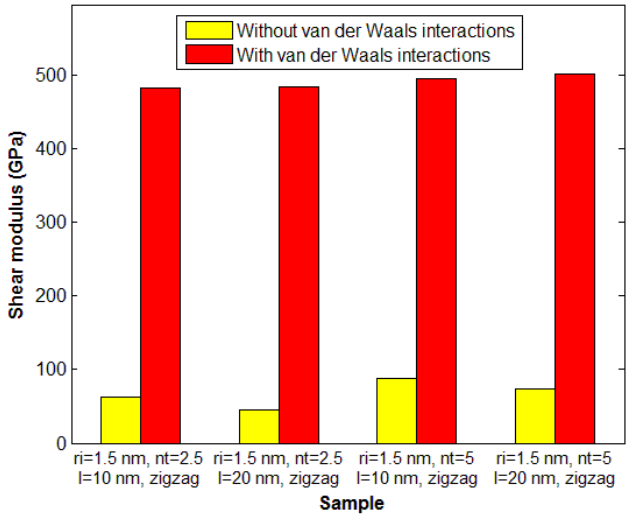

Figure 13: Comparison of shear moduli of sample CNSs with and without van der Waals interactions (r_i is the inner radius, n_t is the number of turns and l is the length of CNS).

Summarizing the results of Figure 12 and 13, one may conclude that with van der Waals interactions being considered, $E = 1100$ GPa and $G = 500$ GPa are typical values for CNS. Again, if we compare these results with the properties of CNTs, we can come to this end that CNSs and CNTs have close elastic properties provided that a wealth of van der Waals bonds are formed between the layers of CNS.

4. Conclusion

In order to expand the mechanical knowledge of nanostructures, in this study the elastic behavior of CNS, a less considered carbon nanostructure, was investigated. First, CNS geometry was generated,

and then based on MSM it was modeled as a 3D structure, and finally using finite element software, its elastic moduli were predicted under two conditions: with and without van der Waals interactions. The results of CNSs without van der Waals forces suggest that for a typical CNS, Young's modulus is about 1040 GPa and shear modulus, being reported for the first time, is around 40-50 GPa. Young's modulus is negligibly affected by CNS geometric parameters (inner radius, number of turns, length and chirality). But shear modulus is notably dependent on number of turns and length of CNS. On the other hand, the results of CNSs with van der Waals bonds imply that for a typical CNS Young's and shear moduli are around 1100 GPa and 500 GPa respectively, regardless of geometric parameters. Therefore van der Waals interactions slightly increase stiffness under tension, while they extremely improve the nanostructure torsional stiffness. Compared to its closed-topology counterpart, i.e. CNT, stiffness of CNS under tension is nearly the same, but under torsion is greatly dependent on van der Waals interactions. Without these interactions, shear modulus of CNS is much lower than that of CNT which is brought about by the existence of free edges. However, once taken into consideration, van der Waals bonds compensate the weakening effect of free edges and prevent the slip between layers of CNS, resulting in a shear modulus close to that of CNT.

Acknowledgement

The first author is grateful to Mrs. Mina Manavi for her kind help, contribution in software handling and admirable patience.

References

[1] L. M. Viculis, J. J. Mack, R. B. Kaner, *Sci.* **2003**, *299*, 1361.

[2] G. Mpourmpakis, E. Tylianakis, G. E. Froudakis, *Nano Lett.* **2007**, *7*, 1893.

[3] X. Shi, N. M. Pugno, Y. Cheng, H. Gao, *Appl. Phys. Lett.* **2009**, *95*, 163113.

[4] X. Shi, N. M. Pugno, H. Gao, *Int. J. Fract.* **2011**, *171*, 163.

[5] X. Shi, Y. Cheng, N. M. Pugno, H. Gao, *Appl. Phys. Lett.* **2010**, *96*, 053115.

[6] F. Zeng, Y. Kuang, G. Liu, R. Liu, Z. Huang, C. Fu, H. Zhou, *Nanoscale* **2012**, *4*, 3997.

[7] X. Shi, N. M. Pugno, H. Gao, *J. Comput. Theor. Nanosci.* **2010**, *7*, 517.

[8] D. Xia, Q. Xue, J. Xie, H. Chen, C. Lv, F. Besenbacher, M. Dong, *Small* **2010**, *6*, 2010.

[9] H. Y. Song, S. F. Geng, M. R. An, X. W. Zha, *J. Appl. Phys.* **2013**, *113*, 164305.

[10] S. F. Braga, V. R. Coluci, S. B. Legoas, R. Giro, D. S. Galvao, R. H. Baughman, *Nano Lett.* **2004**, *4*, 881.

[11] Y. Chen, J. Lu, Z. Gao, *J. Phys. Chem. C* **2007**, *111*, 1625.

[12] X. Shi, N. M. Pugno, H. Gao, *Acta Mech. Solida Sin.* **2010**, *23*, 484.

[13] Z. Zhang, Y. Huang, T. Li, *J. Appl. Phys.* **2012**, *112*, 063515.

[14] C. Li, T. W. Chou, *Int. J. Solids Struct.* **2003**, *40*, 2487.

[15] A. L. Kalamkarov, A. V. Georgiades, S. K. Rokkam, V. P. Veedu, M. N. Ghasemi-Nejhad, *Int. J. Solids Struct.* **2006**, *43*, 6832.

[16] J. R. Xiao, J. W. Gillespie, *Polym. Eng. Sci.* **2006**, *46*, 1051.

[17] J. M. Haile, *Molecular Dynamics Simulation: Elementary Methods*, John Wiley & Sons Inc., USA **1992**.

[18] C. H. Sun, L. C. Yin, F. Li, G. Q. Lu, H. M. Cheng, *Chem. Phys. Lett.* **2005**, *403*, 343.

[19] C. Li, T. W. Chou, *Compos. Sci. Technol.* **2006**, *66*, 2409.

[20] X. Gong, G. Yang, in *Proc. IEEE Int. Conf. Multimedia Technol.*, Hangzhou, China **2011**, 1954.

[21] Y. Cheng, X. Shi, N. M. Pugno, H. Gao, *Phys. E* **2012**, *44*, 955.

[22] J. P. Lu, *Phys. Rev. Lett.* **1997**, *79*, 1297.

[23] M. F. Yu, *J. Eng. Mater. Technol.* **2004**, *126*, 271.

[24] D. Qian, G. J. Wagner, W. K. Liu, M. F. Yu, R. S. Ruoff, *Appl. Mech. Rev.* **2002**, *55*, 495.

[25] E. T. Thostenson, Z. Ren, T. W. Chou, *Compos. Sci. Technol.* **2001**, *61*, 1899.